Chapter 29
Spatial Modeling of Land Cover/Land Use Change and Its Effects on Hydrology Within the Lower Mekong Basin

Kel N. Markert, Robert E. Griffin, Ashutosh S. Limaye, and Richard T. McNider

Abstract The Lower Mekong Basin is an economically and ecologically important region that is vulnerable to effects of climate variability and land cover changes. To effectively develop long-term plans for addressing these changes, responses to climate variability and land cover change must be evaluated. This research aims to investigate how the land cover change will affect hydrologic parameters both spatially and temporally within the Lower Mekong Basin. The research goal is achieved by (1) modeling land cover change for a baseline land cover change scenario as well as changes in land cover with increases in forest or agriculture and (2) using modeled land cover data as inputs into the Variable Infiltration Capacity (VIC) hydrologic model to simulate the changes to the hydrologic system. The VIC model outputs were analyzed against historic values to understand to what degree land cover changes affect the hydrology of the region and where within the region these changes occur. This study found that increasing forest area will slightly decrease discharge and increase evapotranspiration whereas increasing agriculture area increases discharge and decreases evapotranspiration. These findings will benefit the Lower Mekong Basin by supporting individual country, as well as basin-wide,

K.N. Markert (✉)
NASA SERVIR Science Coordination Office, Marshall Space Flight Center,
320 Sparkman Drive, Huntsville, AL, USA

Earth System Science Center, University of Alabama in Huntsville,
320 Sparkman Drive, Huntsville, AL, USA
e-mail: kel.markert@uah.edu

R.E. Griffin • R.T. McNider
Department of Atmospheric Science, University of Alabama in Huntsville,
320 Sparkman Drive, Huntsville, AL, USA

A.S. Limaye
NASA Marshall Space Flight Center,
Huntsville, AL, USA

K.P. Vadrevu et al. (eds.), *Land-Atmospheric Research Applications in South and Southeast Asia*, Springer Remote Sensing/Photogrammetry,
https://doi.org/10.1007/978-3-319-67474-2_29

policy for effective land management for water resources management changes as well as policy for the basin as a whole.

Keywords Land cover changes • Hydrology changes • Lower Mekong Basin

29.1 Introduction

Climate variability and land cover change have been identified as major factors contributing to regional vulnerability within the Lower Mekong Basin (LMB) (Francisco 2008). These changes have implications on key functions of the river such as aquatic ecosystem productivity (Kummu and Sarkkula 2008; Lamberts 2008), transport of sediment and nutrients (Kummu et al. 2006), freshwater supply, and disasters (i.e., flooding). The flow changes are also expected to have an impact on agriculture, including irrigation as well as more traditional agricultural practices such as recession rice (MRC 2010). It is therefore important to understand the possible impact climate variability and land cover change have on the hydrology of the LMB system. Many studies to date have characterized how climate change will alter the discharge of the Mekong River (Keskinen et al. 2010; Lauri et al. 2012). For example, Nijssen et al. (2001a, 2001b) evaluated climate effects on the streamflow of the Mekong Basin in context of global watersheds and found that the Mekong Basin's streamflow will decrease due to climate change. Additionally, more targeted studies into the effects of climate change on the Mekong Basin have been conducted (Eastham et al. 2008; Prathumratana et al. 2008; Kingston et al. 2011; Lauri et al. 2012) concluding that streamflow is highly dependent on changes in precipitation.

Only a limited number of studies have focused on the land cover and Earth surface effects on hydrologic parameters within the Mekong Basin. One such study by Costa-Cabral et al. (2008) investigated the land cover influences on soil moisture and surface runoff. Further studies into the land surface effects on the hydrology of the Mekong Basin were conducted to examine agricultural irrigation effects on water and energy balances (Haddeland et al. 2006a) and on water withdraws and surface energy (Tatsumi and Yamashiki 2015). Other research has been conducted on the effects of land cover change on hydrology outside of the Mekong Basin by coupling land cover change models with hydrologic models. For example, Nagaraj and Yaragal (2008) used the Conversion of Land Use and its Effects at a Small regional extent (CLUE-S) model to investigate the impacts of development scenarios on a watershed. Additionally, Wijesekara et al. (2012) coupled a cellular automata model with the MIKESHE/MIKE 11 hydrologic model to assess the impact of the potential land use changes over next 20 years on the hydrologic process. The integration of land cover change models provide a comprehensive picture of the watershed by incorporating the dominant land use transitions and their impact on the land phase of the hydrologic processes, thus improving the study over the use of a single scenario such as an increase in deforestation or afforestation (Dwarakish and Ganasri 2015).

Few studies have attempted to characterize the changes to the hydrologic system as a whole or analyzed how basin development via land cover change will alter the comprehensive hydrologic regime. This research effort aims to provide critical information on the spatial and temporal variability of multiple hydrologic parameters within the LMB under a variety land cover change scenarios. The results of this research are focused toward enabling decision makers to understand a variety of potential changes to the hydrologic regime influenced by future land cover change for effective land management for water resources management. The overarching goal of the research is to answer the question: How will the land cover change affect the spatial and temporal characteristics of the hydrologic system within the LMB? The research question will be answered through specific objectives including:

1. Develop, calibrate, and validate a land cover change model for the LMB,
2. Setup, calibrate, and validate a hydrologic model for the LMB,
3. Simulate land cover change for different user-defined land cover change scenarios with incremental increases in forested and agricultural areas,
4. Develop a climatological dataset for hydrological variables by simulating the hydrology for the observed climate from 1980 to 2010,
5. Simulate hydrologic parameters for the different land cover change scenarios,
6. Discuss these analyses in detail to provide errors and context for decision making.

29.2 Study Area

The LMB is an economically and ecologically important region located in Southeast Asia spanning five countries: Myanmar, Thailand, Laos, Cambodia, and Vietnam (Fig. 29.1). The main channel of the basin, the Mekong River, is approximately 4735 km in length and is the twelfth longest river in the world. The Lower Mekong portion of the river accounts for 57% of the total channel length, totaling approximately 2700 km. The LMB climate is classified as having a tropical savanna climate and tropical monsoon climate based on the Köppen climate classification (Peel et al. 2007). The hydrology of the region is characterized by a large mean annual discharge concentrated in a regular wet season peak driven by the southwest monsoon from May to October accounting for more than 80% of the annual rainfall in the region (Kite 2001). The seasonal flooding brought by the monsoon largely drives the ecological functions within the region such as fish migration, fish spawning, and vegetative productivity.

The Mekong River Basin supports a population of approximately 70 million people that are projected to increase by 60% in 2050 (Pech and Sunada 2008). The Mekong River Basin not only supports a substantial human population, but also over 500 species of fish with many more land vertebrates, placing it within the top three rivers systems in the world in terms of fish biodiversity (Dudgeon 2000) and

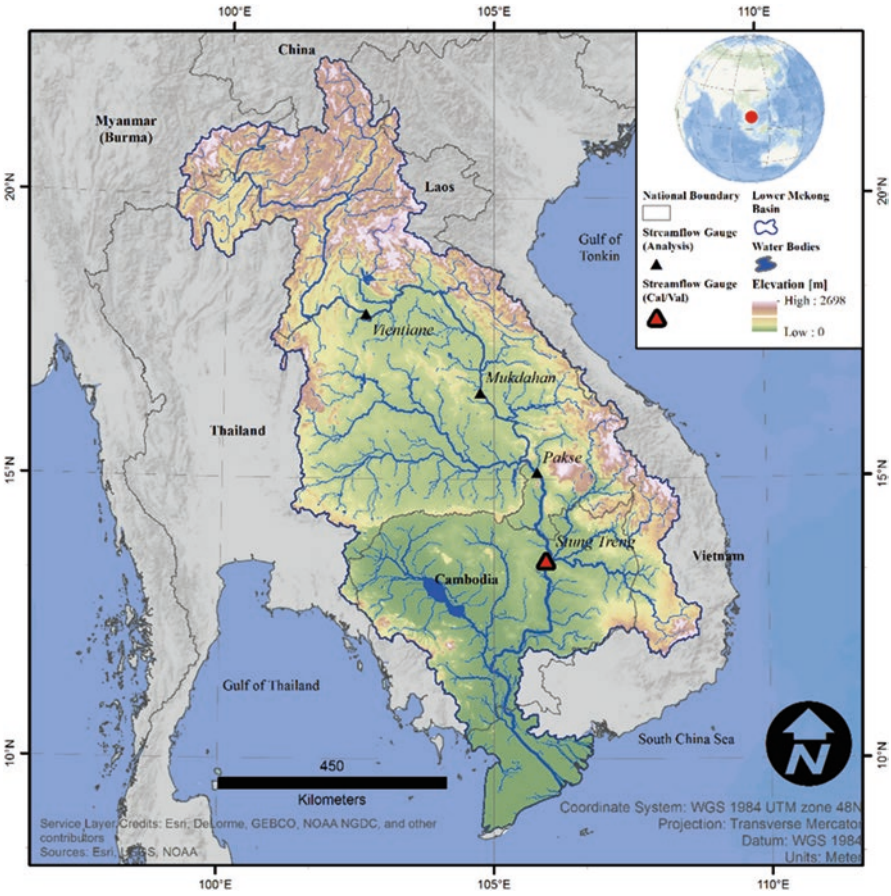

Fig. 29.1 Study area map of the LMB showing the locations of the river gauging stations used in this study overlain a DEM dataset

makes up a large portion of the continent's Indo-Burma biodiversity hotspot (Kityuttachai et al. 2016). Over three-quarters of the population in LMR depends directly or indirectly on agriculture (Kityuttachai et al. 2016) and other economic activities including tourism, agriculture, forestry, fishing, manufacturing, and energy production (Costenbader et al. 2015a). For example, Thailand and Vietnam are the number one and two, respectively, largest exporters of rice in the world (Sakamoto et al. 2006) estimated to be a total of about US$ 703.68 million from 2000 to 2004 (Cong Thanh and Singh 2006).

29.3 Data

29.3.1 Land Surface Data

The data used in this study to represent land cover were the NASA Moderate Resolution Imaging Spectroradiometer (MODIS) combined land cover product version 5.1 (MCD12Q1v5) (Strahler et al. 1999; Friedl et al. 2010; LP DAAC 2010) and the Visible Infrared Imaging Radiometer Suite (VIIRS) surface type environmental data record (ST EDR) (Godin 2014; NOAA 2016). The MCD12Q1v5 dataset is a land cover dataset derived from the MODIS sensors onboard both the Aqua and Terra satellites with a cross-validated accuracy of 74.8% with a 95% confidence interval of 72.3–77.4% accuracy (Friedl et al. 2010). The VIIRS ST EDR dataset is a land cover dataset derived from VIIRS moderate resolution imagery using the MODIS heritage C5.0 decision tree classification algorithm. The ST EDR product is in the beta maturity stage and is currently going through rigorous validation; preliminary validation work shows the dataset currently is below its planned accuracy of 70% (Justice et al. 2013). The land cover scheme that both datasets are provided in is the International Geosphere-Biosphere Programme (IGBP) classification scheme containing 16 classes which were specifically identified to capture the physical characteristics of the surface and primarily to surface vegetation at a global scale (Loveland and Belward 1997). These classes were reclassified to the International Panel on Climate Change (IPCC) land cover classification using a similar reclassification scheme as Al-Hamdan et al. (2017); the only change to the reclassification scheme was for the Woody Savanna class to be remapped as Grassland. Woody Savanna areas have an understory dominated by grasses with a large amount of roots in the top layer of soil which is different than a Forests root system (Ratnam et al. 2011) making a difference in the land surface parameterization for hydrologic modeling. This reclassification resulted in six land cover classes that are consistent with other climate modeling efforts (Milne and Jallow 2003). Additionally, quality control layers provided within the datasets were used to mask out poor quality data to preserve the quality of future analysis using the land cover datasets.

The United States Geological Survey (USGS) Global Multi-resolution Terrain Elevation Data 2010 (GMTED2010) was used as the digital elevation model (DEM) dataset to derive terrain-related variables. This dataset was created through the collaboration of the USGS and the National Geospatial Intelligence Agency using the latest and most accurate datasets and was found to have a root-mean square error (RMSE) between 26 and 30 m (Danielson and Gesch 2011).

Ancillary datasets for the land surface such as major road locations, soil characteristics, and population density were used to derive inputs for more accurate modeling of land use and used as inputs into the hydrologic model. The Global Roads Open Access Data Set version 1 (gROADSv1) acquired from NASA's Socioeconomic Data Applications Center (SEDAC) was used as the data for major

roads and proximity to roads in the land cover change modeling. The Harmonized World Soil Database (HWSD) was used as the data to describe soil characteristics for the hydrologic model (Nachergaele et al. 2012). This dataset is a collection of regional soil databases that have been harmonized and formatted for use in a GIS. Additional ancillary data used as an input for the land cover change modeling included LandScan 2014 population density data developed by Oak Ridge National Laboratory, found to have an accuracy of ±14.5% difference as compared to the validation dataset (Dobson et al. 2000).

29.3.2 Meteorological Data

Meteorological forcing data are required inputs into a hydrological model that are used in the water balance through water and energy calculations. A collection of meteorological reanalysis data and satellite-derived precipitation measurements as well as an observed climate dataset were used as inputs for the hydrologic model parameterization and simulations.

The maximum and minimum surface air temperatures and the wind speed data used to represent the current conditions needed for the meteorological forcings were collected through the National Center for Atmospheric Research (NCAR) Research Data Archive from the European Centre for Medium-Range Weather Forecasts (ECMWF) ERA-Interim reanalysis dataset (ECMWF 2009; Dee et al. 2011; Berrisford et al. 2011). The ERA-Interim reanalysis data were chosen for this study because they were found to be slightly more accurate than other reanalysis datasets when compared to global flux tower observations, particularly for near-surface temperatures and wind speed (Decker et al. 2012). Precipitation errors in the reanalysis data due to premature precipitation onset in the model (Trenberth et al. 2011) and data assimilation methods (Dee et al. 2011) pose a challenge for using the ERA-Interim precipitation data for hydrologic applications; therefore, the Climate Hazards Group Infrared Precipitation with Stations (CHIRPS) dataset was used as the precipitation-forcing data for this study (Funk et al. 2015). The CHIRPS dataset was found to outperform other satellite-derived rainfall datasets at capturing seasonal cycles and has the lowest mean error of all the datasets compared at −3.21 mm (Tote et al. 2015). The WorldClim version 1 observed climate dataset was used in the study of climatic annual averages of meteorological forcing variables such as annual precipitation and average temperature needed for parameterization into the hydrologic model (Hijmans et al. 2005).

29.3.3 Validation/Observed Data

Observed discharge data for the calibration and validation of the hydrological model were acquired from the Mekong River Commission (MRC) database (MRC 2011). This database consists of hydrometeorological data including

discharge, precipitation, and other variables from ground-based stations distributed throughout the Mekong basin. Four discharge stations were selected for use in the analysis of this study shown in Fig. 29.1: Vientiane, Mukdahan, Pakse, and Stung Treng. The Stung Treng gauging station was used for the calibration/validation process as it was found to be the most suitable for calibration being the most downstream observation station with high-quality discharge data. The Kratie station, which is located further downstream, was found to be inadequate for the calibration, validation, and analysis in this study. There are issues in the discharge time series data, most likely induced by gradual changes in river cross-section (Lauri et al. 2012).

29.4 Methods

29.4.1 Land Cover Change Modeling

Land cover projections were modeled using a top-down modeling approach to find the dominant land cover type for a given geographic location within the LMB; this method is based off the Conversion of Land Use and its Effects at Small regional extent (CLUE-S) modeling framework (Verburg et al. 2002). The CLUE-S model framework was chosen for this study because it allows for land cover trends to be altered, simulating policy changes and creating different scenarios of land cover change. This modeling framework is separated into two distinct modules: a non-spatial and spatial module. The non-spatial module calculates the areal change for all land cover types for the basin as a whole which are used to drive the spatial module. Past trends in land cover change were calculated and used to calibrate what are thought to be future trends in land cover change. The future demand for a given land cover class within the region was calculated using linear extrapolation (Pontius and Schneider 2001; Brovkin et al. 2004; Ito 2007). The main drivers of land use change in the past decade comprised of global economic drivers influencing expansion of agriculture and plantation estates, exploitation of minerals and gas, as well as local drivers such as logging, forest fires, high population growth, and other economic and demographic changes including poor governance (Costenbader et al. 2015b). It can be expected that the drivers will influence similar land use change trends in the near future as the region is still experiencing economic growth and with no foreseeable changes in land management policy. Within the spatial module of the model, the calculated demand for a given land cover type is allocated onto a raster grid based on suitability for a land cover occurring at a given location. The suitability map was based on the probability of a given location to be a given land cover type at a given time using a logistic regression model and iterative process to reach the calculated demand for the region. The allocation module was further constrained using logical land cover change decision rules (i.e., certain land cover types can or cannot be converted to another, such as water converting to urban).

29.4.1.1 Land Cover Change Model Validation

To understand the accuracy and errors associated with the land cover model, a validation process was completed. The validation metrics used in the accuracy assessment included computing a confusion matrices for different simulations with associated statistics and qualitatively comparing the two maps for the modeled land cover against the observed to identify if the model captured broad land cover patterns within the region. Three land cover simulations were completed for the validation process: (1) a 5-year projection for 2011, (2) a 5-year projection for 2015, and (3) a 10-year projection for 2015. These simulations were chosen to validate the model because this allowed for two time periods to be modeled with a 5- and 10-year projection providing an understanding of the accuracy under different scenarios.

The confusion matrix and associated statistics were calculated by taking a stratified random sample of 740 points covering all classes to extract the land cover classes from the modeled 2011 and 2015 data as well as the observed MCD12Q1v5 data for 2011 and VIIRS ST data for 2015. The samples were used to create confusion matrices for each simulation shown in Fig. 29.2. It can be noted that the land cover change model correctly classified the majority of the classes. The forest class and water classes had the highest accuracy of prediction. There was, however, difficulty in correctly classifying grassland and agriculture due to similarities between classes (Clay et al. 2016).

Additional metrics were calculated based on the confusion matrices including overall accuracy, producer's accuracy, user's accuracy (Foody 2002; Olofsson et al. 2014), and the kappa statistic (Stehman 1996). These statistical metrics are methods frequently used to assess the agreement between the modeled land cover type and observed land cover type. The summary of the error statistics for 2011, 2015 5-year,

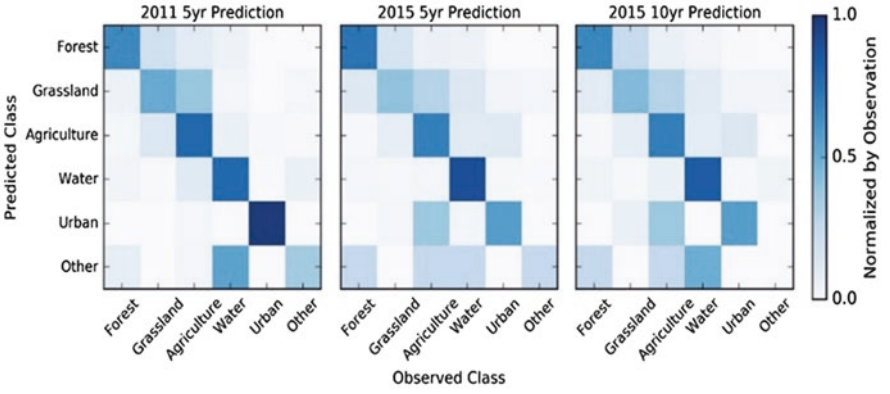

Fig. 29.2 Confusion matrices for the validation of land cover change simulations. From left to right are the 5-year prediction for 2011, 5-year prediction for 2015, and 10-year prediction for 2015. All of the cells were normalized by the observed class

Table 29.1 Summary of the error statistics calculated for the land cover validation simulations

Simulation year	Overall accuracy (%)	Producer's accuracy (%)	User's accuracy (%)	Kappa statistic
2011	71.95	68.00	70.61	0.64
2015 (5 year prediction)	67.97	59.10	55.30	0.57
2015 (10 year prediction)	66.08	53.40	51.32	0.55

and 2015 10-year simulations are provided in Table 29.1. As seen in the table, the 2011 modeled data had the best agreement with the observed data. The model was found to be acceptable based on the derived accuracy statistics as the overall accuracy of the model was near 70%. It was found that all simulations' agreement was over 50% more likely to be due to the model than random chance. The user's accuracy, which is how accurate the data is for a user, was found to be lower than desired, however, the model was still deemed fit. The 2015 5- and 10-year simulations have similar accuracies although the 5-year simulation had slightly better accuracy. It was expected that both 5-year simulations will have similar accuracies as the demand calculated would follow the trends more closely, however, this was not the case. The inconsistencies between the two 5-year simulations can be explained by uncertainties associated with the input data for model initialization and validation as the MODIS dataset was to calibrate and initialize the model simulation but the VIIRS dataset was used to validate the simulations. A first-order analysis was performed to investigate the agreement between the MODIS and VIIRS land cover dataset over the study area resulting in a poor agreement between the two datasets (57% overall accuracy). The disagreement between the two datasets likely caused the decreased accuracy statistics calculated for both of the 2015 simulations.

The resulting land cover simulation datasets were qualitatively compared to the observed datasets to identify the spatial distribution of the land cover classes throughout the basin for the three simulations (2011, 2015 5-year, and 2015 10-year). Figure 29.3 shows the land cover data for the observations and simulations. It can be seen that the land cover change model was able to capture the broad geographic structure of land cover for the region, however, the model had particular trouble with the Grassland class. The Grassland class was largely simulated to be clustered together, when, as seen in the observed data, it is distributed. Additionally, there was a larger amount of grassland area allocated to the northern portion of the basin shown in the transition zones between the forested areas. This error is largely a function of the continuity in the input data used to create the suitability layer for each land cover class that does not capture small-scale changes important to land cover. Additionally, the LMB is a large geographic area with different ecoregions that have different suitabilities for different classes. As such, the model created for this study is optimized to capture the general trends, not specific regional trends within the basin.

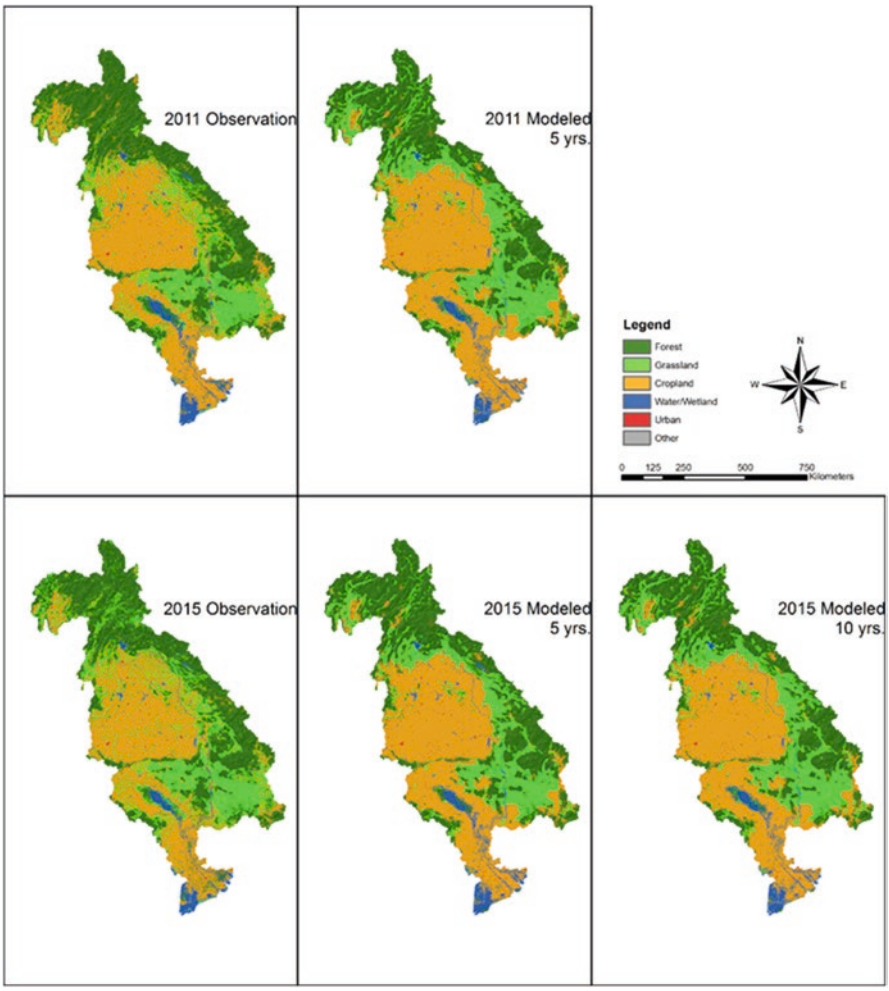

Fig. 29.3 Observed and simulated land cover for the 2011 and 2015 land cover change simulations

29.4.1.2 Land Cover Change Simulations

The future land cover simulations were run at 5-year increments from 2015 to 2050 with multiple scenarios. The first simulation was a baseline scenario; this simulation used the trend lines calculated from the previous land cover data. The modeled land cover for 2020–2050 are assumed to be representative of the future land cover if the current trends were to remain the same. The next few model runs were set up and executed to simulate changes in land cover policy for the LMB that would alter the trends in land cover change. The trends for the Forest and Agriculture classes were both increased to 5 and 10%; a total of four additional scenarios were completed. The forest and agriculture class trend was chosen to be altered to simulate policy

changes of the two classes within the region. The trend increases of 5 and 10% were chosen to understand the sensitivity of larger increases of the land cover type to the hydrologic system.

29.4.2 Hydrologic Modeling

The Variable Infiltration Capacity (VIC) model was employed for this study to simulate hydrologic parameters spatially throughout the Lower Mekong Basin. The VIC model is a macroscale semi-distributed model that solves energy and mass balance at each grid cell to simulate evapotranspiration, interception, surface runoff, baseflow, and other hydrological fluxes (Liang et al. 1994). Each grid cell is simulated independently and able to be partitioned into multiple vegetation heterogeneities, multiple soil layers with variable infiltration rates, and topography layers. The model allows for the time step to update fluxes and for model states to be defined as daily or sub-daily increments. The VIC model does not represent deep groundwater or water stored in bedrock and this parameter is not considered within this study. The VIC model is coupled with a routing model to simulate discharge using the surface runoff and baseflow parameters. This study uses the routing model described by Lohmann et al. (1996, 1998) to route the streamflow from each grid to a specified outlet.

The VIC model has been successfully implemented in hydrologic studies for major river basins in the US (Abdulla et al. 1996; Bowling et al. 2004; Bowling and Lettenmaier 2010), the Mekong Basin (Costa-Cabral et al. 2008; Haddeland et al. 2006a, 2006b), and globally (Nijssen et al. 2001a, 2001b, 2001c). Additional studies have employed the VIC model to study specific aspects of the hydrologic cycle such as changes in evapotranspiration over time (Liu et al. 2013a) and changes to land use change (Cuo et al. 2011; Matheussen et al. 2000) making it a well-established model in hydrological research.

The model was executed at 0.1 degree resolution for the LMB with sub-grid land cover and elevation was defined within each grid cell to account for small-scale variability within the large grid cells for a better representation of the land surface. The routing model was applied at a daily time step and then averaged monthly resulting in simulated monthly average discharge. The VIC model was used to simulate surface runoff, baseflow, and evapotranspiration hydrologic parameters for this study from 1982 to 2010 as a baseline climatology and for 5-year increments from 2020 to 2050 to assess changes due to climate variability.

29.4.2.1 Model Calibration/Validation

The baseline climatology simulation was partitioned into two additional sections: calibration (1982–1990) and validation (1991–2004). The calibration/validation process was performed graphically and statistically comparing simulated

discharge against observed discharge. The observed discharge dataset was acquired from the Mekong River Commission (MRC 2011) for the gauge shown in Fig. 29.4a, b.

The model evaluation guidelines from Moriasi et al. (2007) were followed when assessing the performance of the hydrologic model. The model evaluation guide recommends using the Nash-Sutcliffe Model Efficiency Coefficient (NSE) (Nash and Sutcliffe 1970), RMSE-Standard Deviation Ration (RSR), and Percent Bias (PBIAS) when evaluating the model (Moriasi et al. 2007). Additional statistics used in this study to evaluate the model include Pearson correlation coefficient (R) and Mean Relative Error (MRE). Figure 29.4 displays the monthly average discharge for the calibration (a) and validation (b) periods. The hydrographs show an overall good agreement between the simulated and observed discharge; however, the model does slightly over predict baseflow during the dry season. This anomaly becomes less pronounced in the later years, particularly around 2001 which is the date of the land cover data used to parameterize the model. This over prediction of baseflow can be attributed to the land cover parameterization, which does not affect the overall result of the simulation.

The overall statistical analysis show that the model performance is "good" to "very good" for simulating monthly average discharge based on the Moriasi et al.

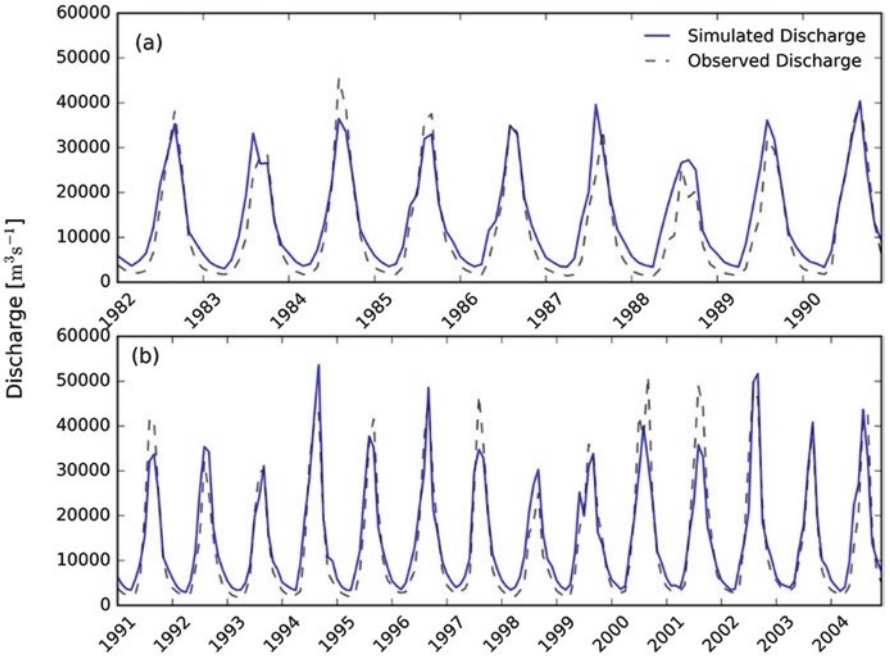

Fig. 29.4 Calibration/validation hydrographs for the discharge gauge in the LMB. The calibration period, 1982–1990, is shown on the top plot (**a**) and the validation period, 1991–2005, is shown on the bottom (**b**)

Table 29.2 Summary of error statistics for the hydrologic model calibration and validation process

Statistic	R [−]	NSE [−]	PBIAS [%]	RSR [−]	MRE [%]
Calibration	0.96	0.87	−20.70	0.28	68.13
Validation	0.95	0.89	−7.40	0.24	41.95

(2007) performance guidelines. The calculated error statistics, summarized in Table 29.2 for both the calibration and validation periods, are comparable to other modeling efforts for the Mekong Basin. In a study by Thompson et al. (2013), a NSE of 0.791 and 0.858 was calculated for two different gauging stations within the basin, Nakhon Phanom and Pakse, respectively. Additionally, Kingston et al. (2011) obtained a NSE value of 0.770 for the Pakse station. Although the model performance statistics derived from other studies are not directly comparable to the error statistics from this study because of differences in models used, calibration/validation periods, and gauging stations, they provide a baseline for what constitutes an acceptable model within the region.

29.4.2.2 Hydrologic Simulations

The hydrologic simulations were run at 5-year increments from 2015 to 2050 to analyze how land cover change affects the hydrologic system. The simulated land cover change data outlined in Sect. 29.4.1.2 were used as the land cover data input for the hydrologic model during the specified time periods. In total, there were five land cover scenarios to analyze the effects of land cover change on the hydrology. The meteorological data used for the land cover change hydrologic simulations were the observed data from 2000 to 2001. The meteorological data range was chosen to remain constant with the land cover control time frame. The meteorological forcing remained constant for the land cover hydrologic simulations to be confident that the identified hydrologic changes were due to land cover change.

29.4.3 Hydrologic Change Analysis

29.4.3.1 Discharge Changes

An analysis was performed to understand the effects climate variability and land cover change have on the flow regime at gauging stations along the river (Fig. 29.1). The analysis comprised of simply finding the percent difference of the hydrologic projection simulations compared to the climatic average from 1981 to 2010, defined by Eq. 29.1

$$\%\Delta = \frac{\left[\mu(Q_s) - \mu(Q_c)\right]}{\mu(Q_c)} \cdot 100 \tag{29.1}$$

where $\%\Delta$ is the percent difference, $\mu(D)$ is the yearly average streamflow for the simulation (s) and control (c). It should be noted that the control used in this equation is the data from a historic hydrologic simulation using the same meteorological inputs. When applying the equation to understand the change due to climate variability, the control data used were the simulation using the bias-corrected climate reanalysis data from 1981 to 2010. In contrast, when analyzing the change due to land cover change, the control data used was the hydrologic simulation using the observed meteorological data from 1981 to 2010. The hydrologic simulation data were used instead of the observed streamflow data to limit errors in the results that could emerge from comparing modeled data with uncertainties to observed data.

29.4.3.2 Seasonality Analysis

A seasonality analysis was employed to complement the previous analysis in identifying the changes to the timing of the flow regime at the gauging stations (Fig. 29.1). This analysis identified the mean date of the wet season and variability of occurrence of extreme events based on the Burn index (Burn 1997) which uses circular statistics to identify the mean date or peak of the season and intensity of the season (Parajka et al. 2009). The mean date of occurrence represents an average position of event occurrences which are plotted in polar coordinate on a unit circle. The position of the event occurrences for each month can be found using Eq. 29.2

$$\Theta_i = D\,2\pi\,/\,12 \tag{29.2}$$

where D is the mean date for each month, i, for example D for January and December is 16 and 350, respectively. The direction of the mean date is calculated using the following sequence of Eqs. 29.3–29.5

$$\bar{x} = \sum_{n}^{i=1} \cos(\Theta_i)\,/\,n \tag{29.3}$$

$$\bar{y} = \sum_{n}^{i=1} \sin(\Theta_i)\,/\,n \tag{29.4}$$

$$\bar{\Theta} = \tan^{-1}\left(\bar{y}\,/\,\bar{x}\right) \tag{29.5}$$

where $\bar{\Theta}$ is the direction of the average vector from the origin representing the mean date of occurrence of extreme events. The variability or intensity of the season is characterized by a length parameter defined in Eq. 29.6

$$r = \sqrt{\bar{x}^2 + \bar{y}^2}\,/n \tag{29.6}$$

where r ranges from zero to one, with zero representing a uniform distribution and one representing all of the extreme events occur in the same month. This analysis provides an understanding of how the mean date and intensity of the wet season of the LMB change due to climate variability and the changes in land cover.

29.4.3.3 Runoff Elasticity

In this study, the effects of land cover change on surface runoff were estimated with the concept of elasticity. Numerous studies have documented the sensitivity of streamflow to climate change by estimating the precipitation elasticity of streamflow. Schaake (1990) introduced the concept of elasticity for evaluating the sensitivity of streamflow to changes in climate. Climate elasticity of streamflow is defined by the proportional change in streamflow Q divided by the proportional change in a climatic variable such as precipitation P defined in Eq. 29.7.

$$\varepsilon_P\left(P,Q\right) = \frac{dQ/Q}{dP/P} = \frac{dQ}{dP}\frac{P}{Q} \tag{29.7}$$

If the elasticity coefficient is greater than 1, a 1% change in annual rainfall would result in more than 1% change in annual streamflow. For example, an elasticity of +5 indicates that a 1% increase in annual rainfall would lead to 5% increase in annual streamflow.

The principle of elasticity was also applied to the hydrologic simulations with the land cover change scenario data. The same concept is used where the land cover elasticity, εL, was defined as a ratio of the annual runoff to the percentage of a land cover change. If the elasticity parameter is greater than 1, a 1% change in the land cover type will result in a greater than a 1% change in annual runoff. The elasticity parameter for land cover change was calculated using Eq. 29.8 following the methods outlined by Zheng et al. (2013)

$$\varepsilon_L = \frac{\left(R_{(t+1)} - R_t\right)/R_t}{\left(L_{u,(t+1)} - L_{u,t}\right)/L_t} = \frac{\Delta R_t / R_t}{\Delta L_t / L_t} \tag{29.8}$$

where is the sensitivity of annual runoff, R, to changes for a given land cover class, L_u, for two consecutive time periods (t) and (t + 1). The values of elasticity with respect to both the climate and land cover were calculated at the time steps coinciding with the simulations.

29.4.3.4 Spatial Hydrologic Trends

A trend analysis was conducted to understand the changes in yearly accumulated water balance terms throughout time due to either climate variability or land cover change. Furthermore, this analysis was applied spatially throughout the LMB to characterize the geographic variations of the variables. The magnitude of trends was calculated using a nonparametric slope estimator proposed by Sen (1968), where the median slope is calculated among all lines through pairs of two-dimensional sample points. The Sen slope estimator has been used widely to asses trends in climatological (Romanic et al. 2015), hydrologic (Kibria et al. 2016), and remote sensing (Fernandes and Leblanc 2005; Liu et al. 2015) studies by applying Eq. 29.9

$$\beta = \text{median}\left(\frac{Y_j - Y_i}{X_j - X_i}\right) \tag{29.9}$$

where is the median for all possible combinations of pairs of any two data points (i) and (j) in the entire dataset. The median slope is then used to calculate the percent change trend using Eq. 29.10 as explained by Liu et al. (2013a)

$$\%\Delta = \frac{\beta_{x,i} \cdot n}{\mu_{x,i}} \tag{29.10}$$

where is the trend line for the hydrologic variable (x) at pixel (i), n is the number of years for the trend period (for this study it was 40 years, 2011–2050), and was the climatological mean for the variable at a given pixel. The trend estimation was applied to each time series for all of the pixels within the basin and for each hydrologic parameter which included change in storage, runoff ratio, and evapotranspiration. These hydrologic parameters were chosen as they further define the nature of water balance within the system. Characterizing the trends in these parameters will further elucidate how much and where the climate variability and land cover changes alter the hydrologic system. A simple water balance model is used to calculate the change in storage parameter (ΔS) at each grid cell defined as

$$P = E + R + \Delta S \tag{29.11}$$

where P is precipitation, E is evapotranspiration, R is a runoff, and ΔS is the change in storage. The ΔS term is understood to include all of the water stored as soil moisture, snow, and canopy infiltration. Over a long period of time (i.e., 10 years+), it is reasonable to assume that the term ΔS approaches is zero based on conservation of mass (Liu et al. 2013b); however, the short-term water balance and trends are variable. Runoff ratio is defined using Eq. 29.12

$$\alpha = \frac{R}{P} \tag{29.12}$$

where α is the runoff ratio, R is a runoff, and P is the precipitation. Runoff ratio represents the long-term water balance separation between water that is released from the catchment as streamflow or as evapotranspiration, assuming there is no net change in storage. A high value for runoff ratio relates to the region where a large amount of water exits as runoff, whereas a low runoff ration relates to the large amount of water leaving as evapotranspiration. The last hydrologic parameter, evapotranspiration, was output directly from the hydrologic simulations.

29.5 Results and Discussion

29.5.1 Land Cover Change Simulations

The land cover simulations were run specifically to create land cover scenario data as inputs into the hydrologic model. First, before discussing the results of the hydrologic simulations, it is important to discuss the land cover data models to better understand the results of the hydrologic simulations. Specific scenarios were simulated with the land cover model: (a) baseline land cover change (LCC), (b) forest increase of 5%, (c) forest increase of 10%, (d) agriculture increase of 5%, and (e) agriculture increase of

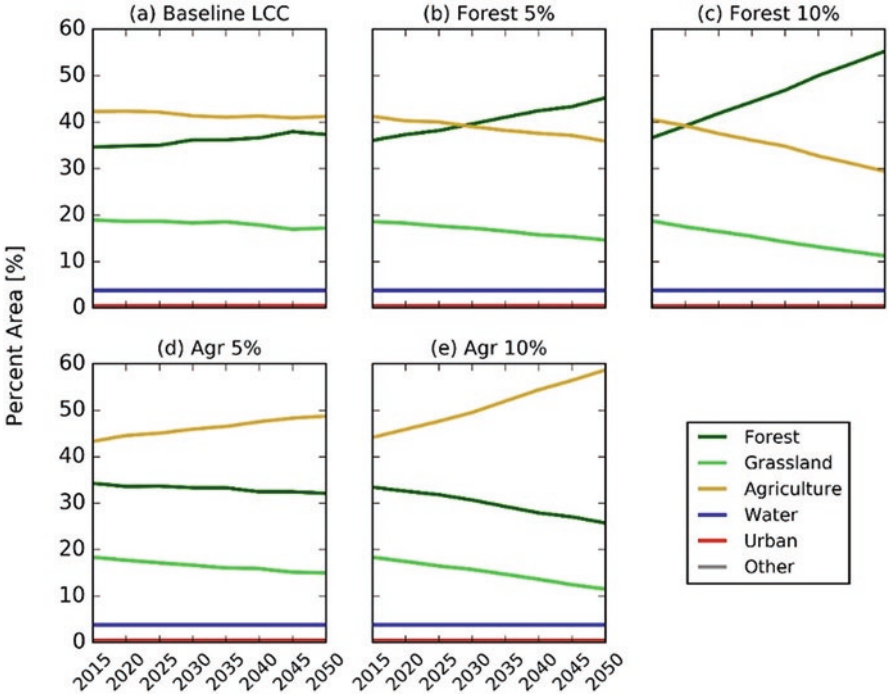

Fig. 29.5 Summary of land cover change simulation areal changes for each class through time

10%. Figure 29.5 displays the results of the land cover change simulations, showing the percent area of each class within the LMB for each time step for all of the simulations. The baseline simulation showed little changes throughout time, however, the other simulations showed rapid increases in the class projected to increase where grassland and the other majority class (forest or agriculture) decreased.

Figure 29.6 shows the spatial distributions for each class under all scenarios for 2050. It can be seen in the maps that the large-scale spatial patterns are consistent, however, with forest increases large patches of forest can be noted where agriculture typically was located and vice versa for the agriculture increases. This shift between the two classes is largely identified in the Cambodia region. It may seem that the scenarios with 10% increases in either forest or agriculture are not feasible but it is important to simulate the hydrologic response to these changes to understand the sensitivity to large shifts in land cover.

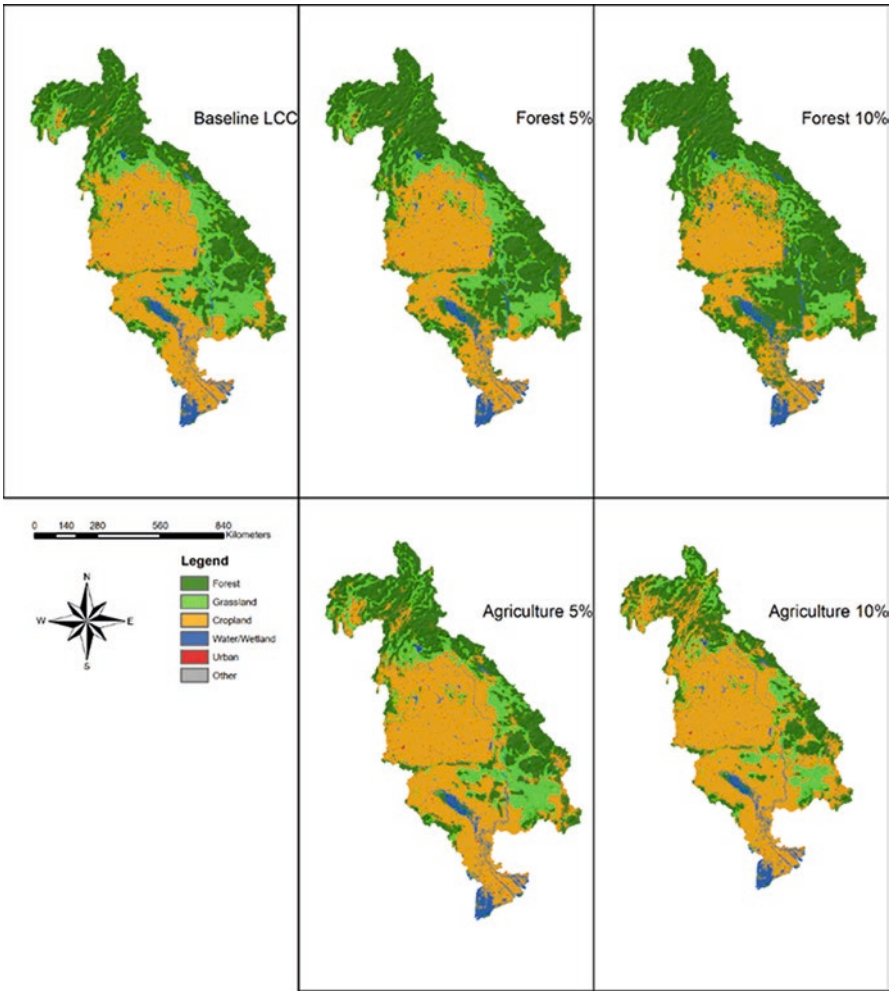

Fig. 29.6 Maps of the resulting land cover change simulations for 2050

The resulting maps and information from the land cover change simulations can be used by land managers and policy makers to help create manageable and advantageous policies for land cover change as well as understand where the land cover change will occur following policy implementation. Based on the modeling, it can be expected to see the greatest land cover change in the lower portions of the basin in and around Cambodia. These changes can have implications for flooding within the flood plains in the region but will not have much contribution to the streamflow in the upper reaches of the basin.

29.5.2 Discharge Changes

The first analysis in addressing changes of the hydrologic system was to evaluate changes to discharge for the gauging stations. Figure 29.7 displays the simulated monthly discharge for 2050 from all of the simulations. The simulation with the climate data showed the greatest change with the peak discharge occurring in July with comparatively minimal wet season discharge following July. The land cover change scenarios showed little changes from the historic average; however, it can be seen that increases in agriculture land increase discharge and increases in forest land decrease discharge.

Additional data were compiled for each gauging station at each year. Figure 29.8 displays the percent difference from mean annual discharge for each scenario. The climate scenario has the greatest impact on the discharge for all stations. Additionally, the land cover simulations show similar trends with agriculture increases resulting in an increase in discharge and forest increases resulting in decreases in discharge.

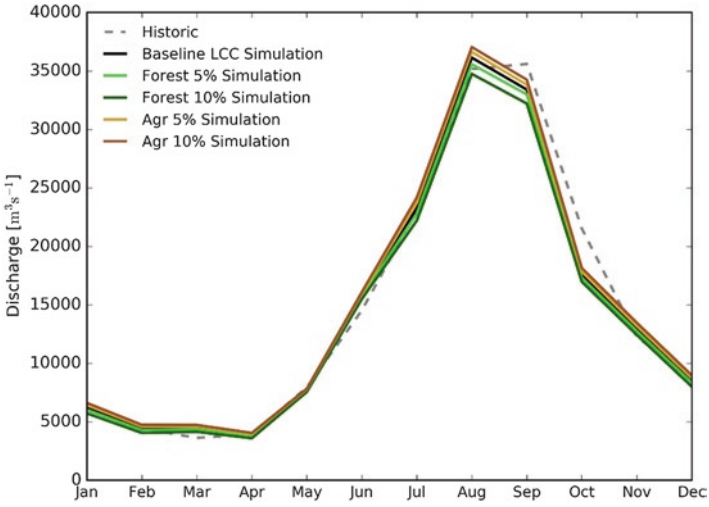

Fig. 29.7 Hydrographs for Stung Treng station showing changes to discharge for 2050 from all of the scenarios

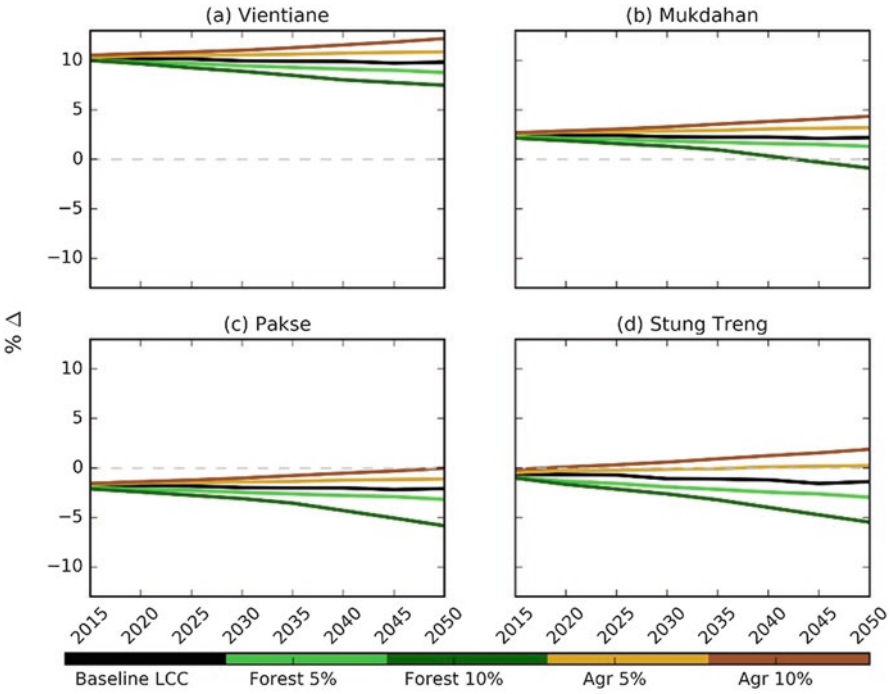

Fig. 29.8 Percent changes in mean annual discharge from all scenarios through time

The decreases in discharge due to increases in forest area are likely due to the fact that increasing the forest area also increases the evapotranspiration for the region. Controversially, by increasing agricultural areas there is a decrease in plant water uptake and vegetation canopy interception which leads to a decreased evapotranspiration and increased runoff. Showing that increases in the forest can decrease discharge throughout the basin has implications for reducing the annual flood waters. The offset in simulated discharge from the land cover scenarios compared to the mean discharge for 2015 at the Vientiane station is most likely due to errors in the spatial allocation of land cover class within the land cover change model upstream from that gauging station, the other stations seem to not have any uncertainties from the hydrologic simulations using land cover scenario data. Additional uncertainties in the discharge separation could be attributed to the upper catchment having an increase in precipitation for 2001 as compared to the climatological average.

29.5.3 Seasonality Analysis

The seasonality analysis was applied to the simulated discharge from the hydrologic simulations using the land cover change scenarios. The results of the analyses are found in Figs. 29.9, 29.10, 29.11, 29.12, and 29.13. As shown in the figures, there was no noticeable difference in seasonality for all land cover change simulations.

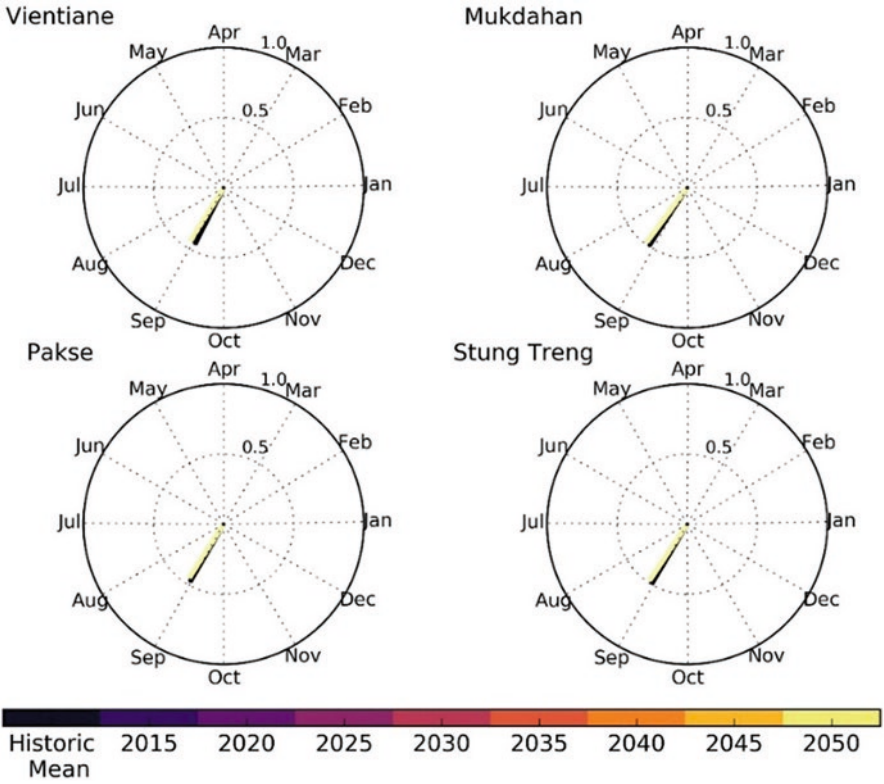

Fig. 29.9 Streamflow seasonality analysis using the baseline land cover change scenario data. Almost no changes in seasonality can be observed due to baseline land cover change scenario

There is a slight shift forward in the mean date of the season, however, the signal is seen in all land cover change scenarios and can be attributed to using meteorological data from 2001 in the simulations and comparing to a climatological mean. It can be deduced from these results that land cover does not have a significant role in seasonality and the region can expect the same onset and intensity of the wet season discharge as has been historically observed under different land cover change scenarios.

29.5.4 Runoff Elasticity

The runoff elasticity due to land cover change for the basin as a whole is summarized in Fig. 29.14. The elasticity calculations due to land cover change could not have a spatial component to the results as the analysis is based on total basin-wide changes for each land cover. For each scenario and land cover class, there is little

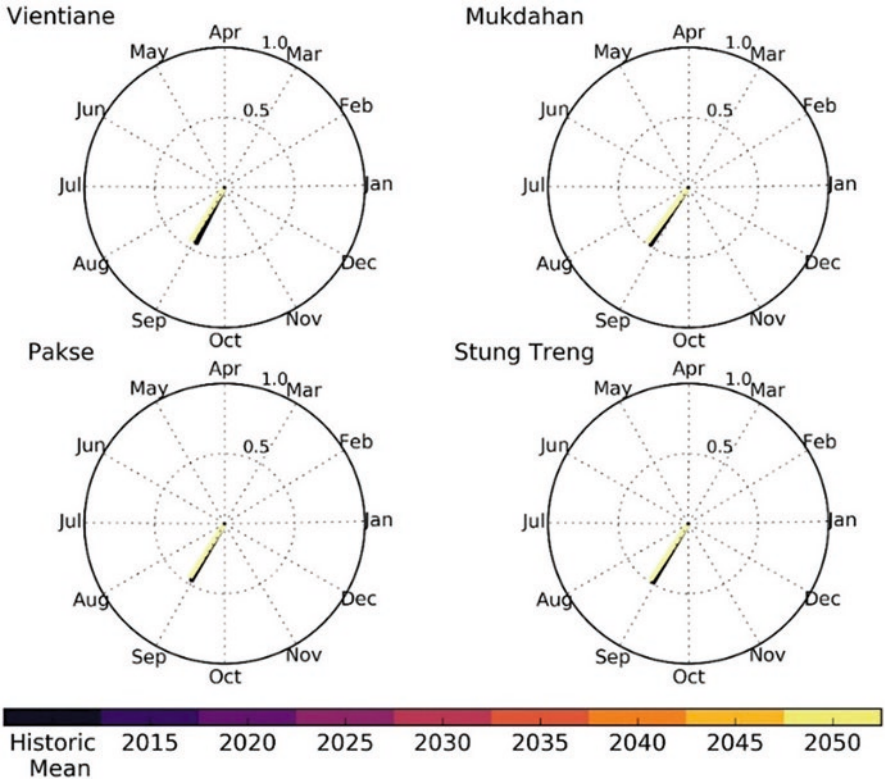

Fig. 29.10 Streamflow seasonality analysis using the 5% increase in forest area scenario

change in the basin-wide runoff. These results align with the findings from the discharge change analysis, where little changes were found in discharge due to land cover change. Conceptually, this is logical as changes in the runoff will result in changes in discharge. There is a small signal (less than 1% change) from both water bodies and urban areas. Interestingly, the urban signals for the 10% increases in forest and agriculture scenarios have similar curves; more research is needed to understand if these curves are actual signals or noise due to the modeling methodologies.

29.5.5 Spatial Hydrologic Trends

The trends for the simulated hydrologic variables due to land cover change are shown in Figs. 29.15, 29.16, 29.17, 29.18, and 29.19.

There are few geographically isolated trends within the basin due to different land cover change scenarios; however, the basin as a whole shows minimal changes

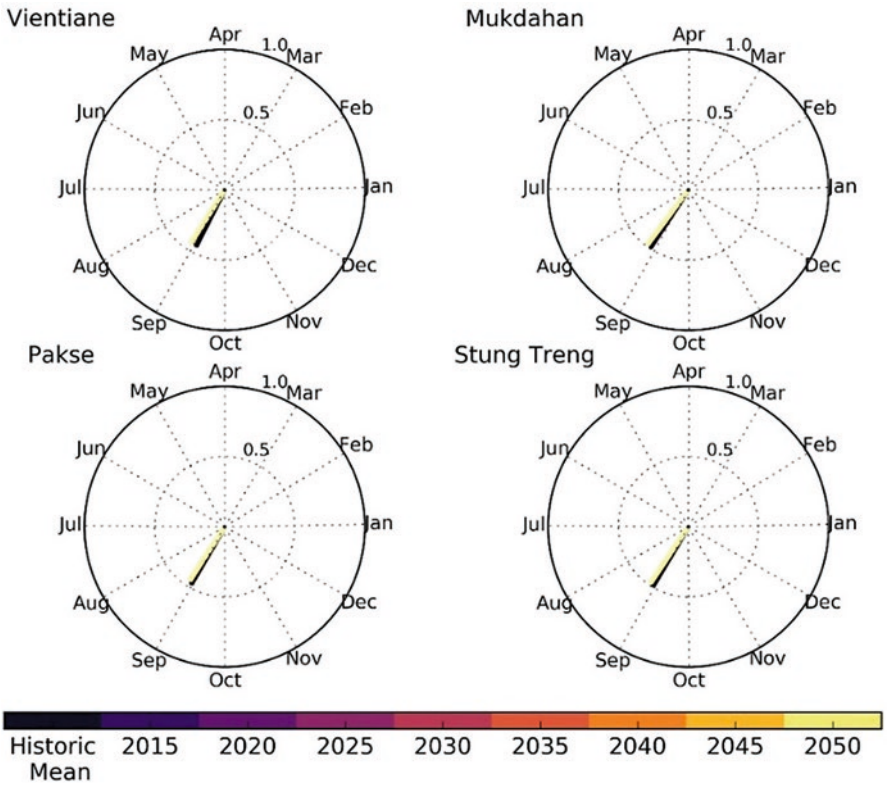

Fig. 29.11 Streamflow seasonality analysis using the 10% increase in forest area scenario

to the hydrologic variables through time due to land cover change. The baseline land cover change scenario shows there is a decreasing trend in storage near the northwestern portions of the basin; additionally, there are small increasing trends in storage in a southeastern portion of the basin. There are no large (greater than 10%) trends for in RP and ET for the baseline land cover change scenario. The increases in forest areas show more of a signal for trends where increases in storage and ET can be seen in both forest scenarios. There is a larger geographic area with increasing trends in storage and ET for the 10% increase scenario due to the increased forest area. The scenarios with increases in agricultural areas show decreasing trends in storage and ET. The findings align with the hypothesis that forested areas in this region would increase overall ET and hold more water and increases in agricultural areas would decrease overall ET and storage. There were no notable changes to the RP variable due to land cover change. Additionally, there seemed to be more intense, 5–25% as opposed to less than 10% change, for increasing trends due to increases in forest area than the decreasing trends of agriculture area, leading to a belief that the hydrologic system of the LMB is more sensitive to increases in the forest area.

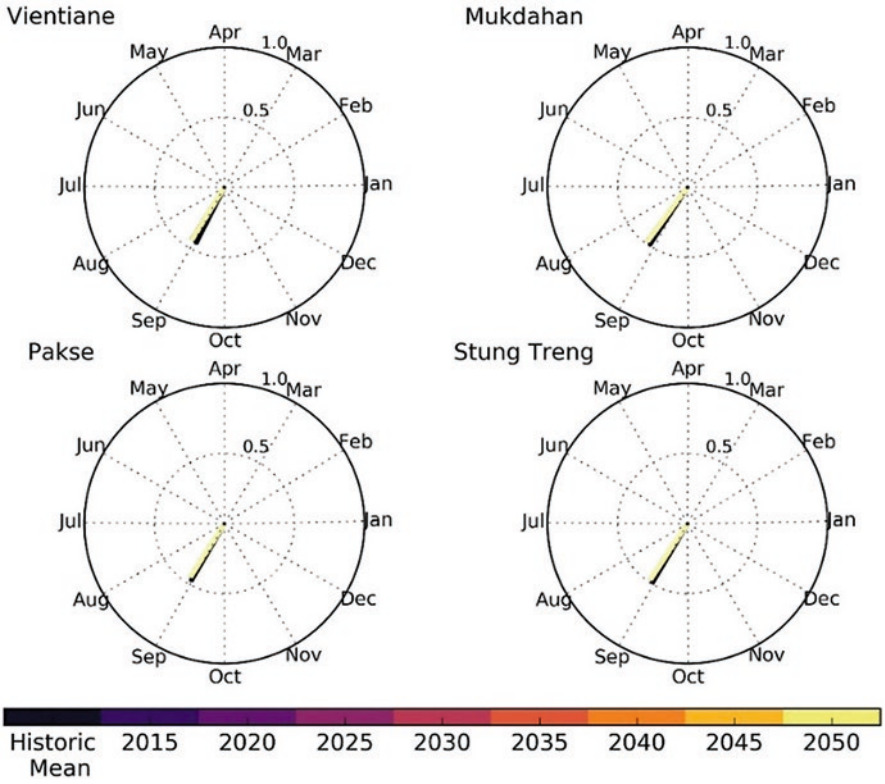

Fig. 29.12 Streamflow seasonality analysis using the 5% increase in agriculture area scenario

29.6 Summary and Conclusions

This study aimed to investigate the spatial and temporal change to the LMB hydrologic system due to climate variability and land cover change. A land cover change model was developed to simulate how the land cover will change through time within the basin under a variety of scenarios. A hydrologic model was setup for the LMB using the VIC hydrologic model. The land cover data from the simulations were used to simulate future hydrologic variables for the basin. The hydrologic variables were then compared to the past climatological averages to analyze for change.

This study used projected land cover within the analysis to test changes to the system due to land cover change. The effects of land cover change on the hydrologic system could be characterized by analyzing past observed data; however, the modeling approach used allowed for land cover change scenarios to be defined, such as the 10% increase in forested area, and analyzed for changes to the hydrologic system. The use of different scenarios could not be achieved using part

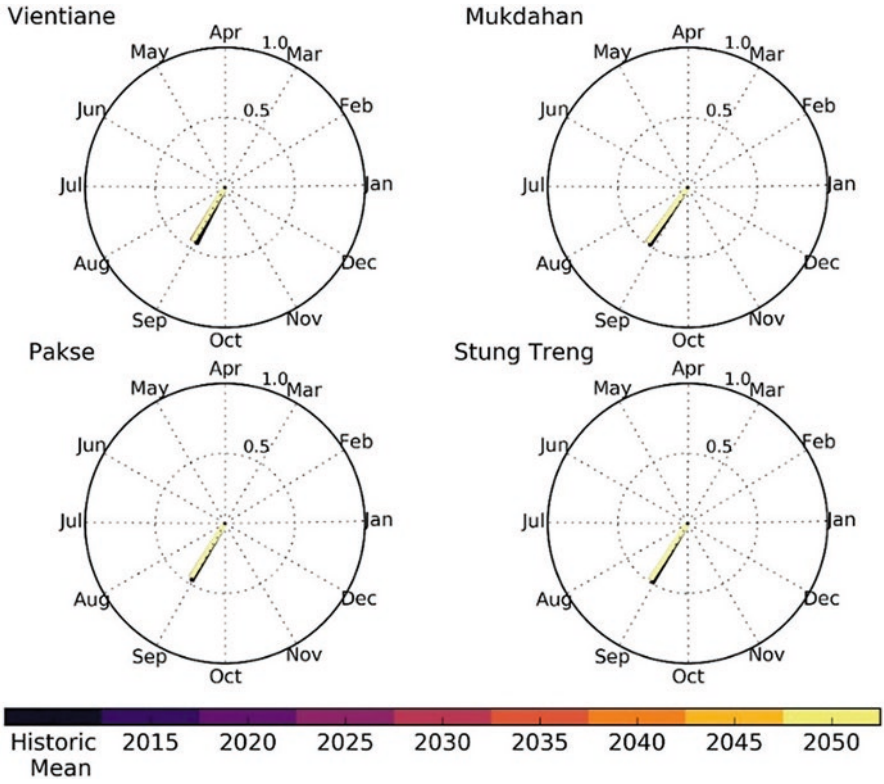

Fig. 29.13 Streamflow seasonality analysis using the 10% increase in agriculture area scenario

observed data; however, using past observed land cover change information would have eliminated uncertainties in results from using modeled data as inputs.

The changes due to land cover were shown to have minimal impacts on the discharge for the entire basin. Although the changes were small, there was a notable separation between the simulated discharge from the forest and agricultural area increases for the land cover change simulations. The forest increases were shown to have a decrease in discharge whereas increases in agriculture areas increased discharge. There was no notable change in the seasonality of discharge due to land cover change. The basin was also found to have almost no sensitivity of surface runoff to land cover changes, making the argument that another variable was controlling the changes in discharge. The spatial trends in hydrologic variables show that storage and evapotranspiration had the most changes due to land cover change, coinciding with the transitions of land cover types. There was an increasing trend in storage and evapotranspiration with increase in the forested area and a decreasing trend in storage and evapotranspiration with increases in the agricultural area. Overall, the largest signal hydrologic system due to land cover change was found to be from changes in evapotranspiration and land surface storage of water which affected the downstream discharge.

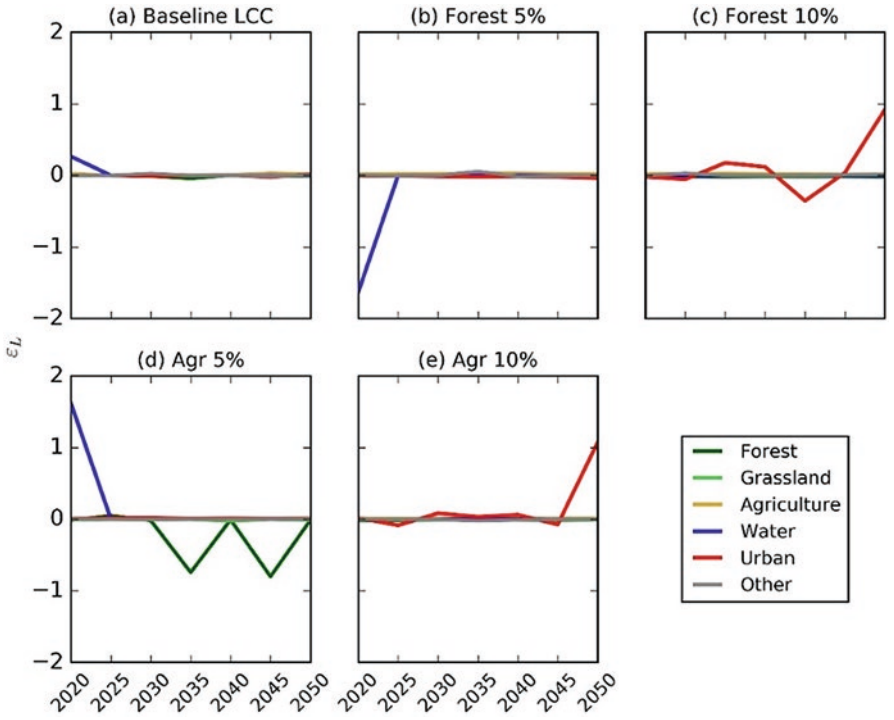

Fig. 29.14 Runoff elasticity values for each land cover class for each land cover scenario. Almost no changes can be seen for each land cover variable through time with small signals (<1%) for the Urban class

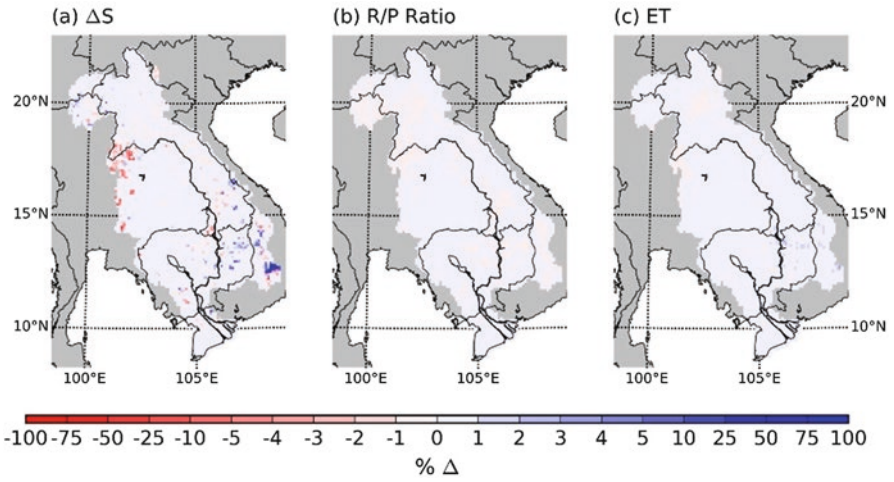

Fig. 29.15 Trends in hydrologic variables in the LMB due to land cover change for the baseline scenario. Minimal changes (both 5–10% increase and decrease) can be seen in ΔS variable across the basin with almost no change in R/P ratio and ET due to the baseline land cover change scenario

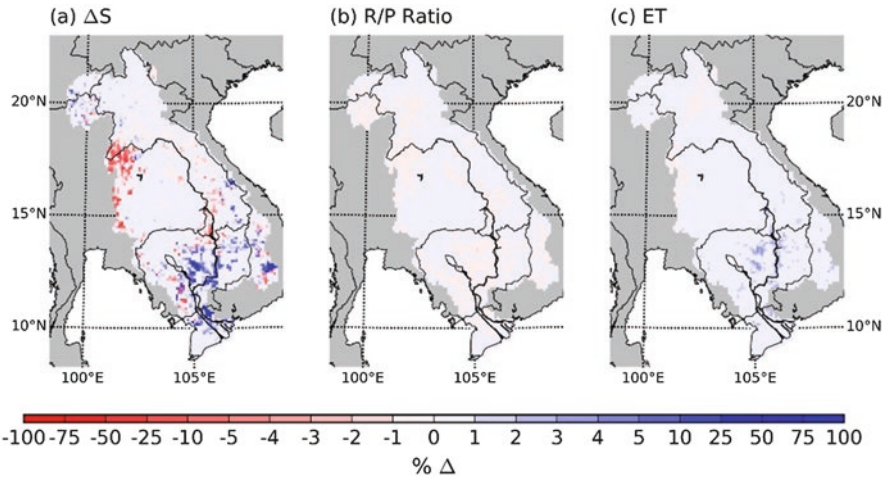

Fig. 29.16 Trends in hydrologic variables in the LMB due to land cover change for the 5% forest increase scenario. Increases in ΔS and slight increases (2–5%) ET can be seen in the southern portions of the basin with the increases in forested area

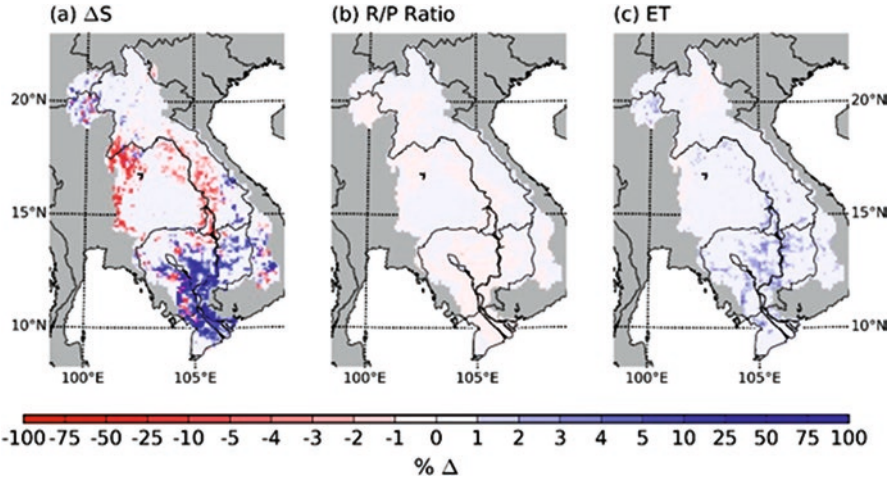

Fig. 29.17 Trends in hydrologic variables in the LMB due to land cover change for the 10% forest increase scenario. Large increases (25–75%) in ΔS and increases (2–5%) ET can be seen in the southern portions of the basin with the increases in forested area; areas increasing are larger for a 10% increase in forest than with a 5% increase in forest

A more significant contribution of this study is the modeling framework that was developed. A calibrated and validated land cover change and hydrologic model have been developed for the LMB which can be used and expanded for other studies. The land cover change model can be applied by land managers to analyze different land cover change scenarios for the basin to understand how policy

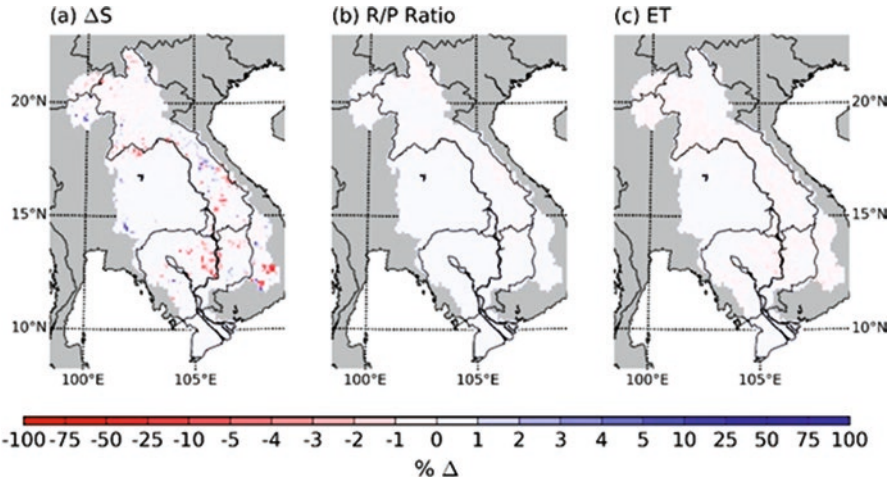

Fig. 29.18 Trends in hydrologic variables in the LMB due to land cover change for the 5% agriculture increase scenario. Slight decreases (−25 to −3%) in Δ*S* can be seen, however, almost no change in *R*/*P* ratio and ET are seen

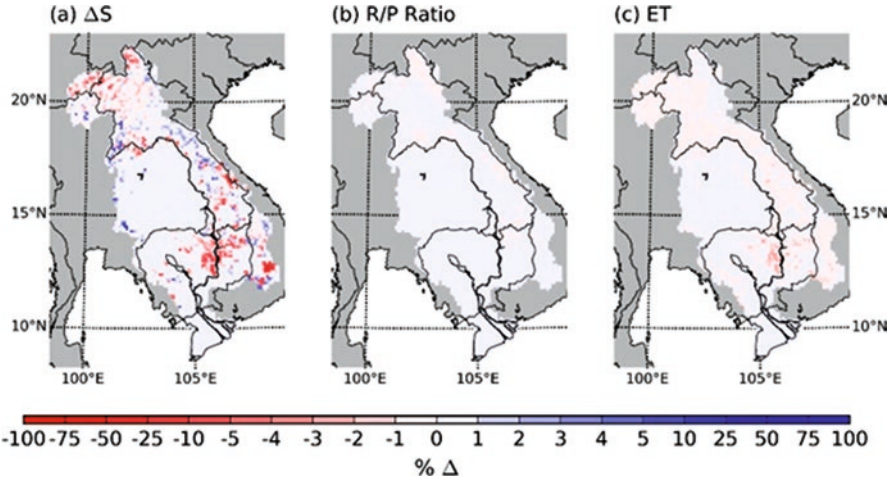

Fig. 29.19 Trends in hydrologic variables in the LMB due to land cover change for the 10% agriculture increase scenario. Slight decreases (−25 to 5%) and minimal increases (1 to 5%) in Δ*S* can be seen with minimal decreases (−5 to −1%) in ET are seen as well

changes may affect the landscape of the basin. The hydrologic model can also be used for future hydrologic research and other weather and climate studies that have a need for the implementation of a land surface model. Furthermore, with the increasing accuracy of data inputs and the expansion of the land cover model, such as representing human decision making and policy changes through agent-based modeling, a more precise depiction of hydrologic changes can be concluded from the modeling efforts.

Acknowledgments The authors wish to thank the Mekong River Commission for supplying the observed discharge data used in this study. A special thanks goes to Faisal Hossain for his assistance with setting up the hydrologic model. The authors are grateful to Dan Irwin, Eric Anderson, Africa Flores, Lee Ellenburg, Larry Carey, Maury Estes, and others for their support and valuable comments. This work was funded through the NASA-SERVIR program part of the Capacity Building program of NASA Applied Sciences as part of K.N.M. graduate work.

References

Abdulla FA, Lettenmaier DP, Wood EF, Smith JA (1996) Application of a macroscale hydrologic model to estimate the water balance of the Arkansas–Red River Basin. J Geophys Res 101:7449–7459

Al-Hamdan MZ et al (2017) Evaluating land cover changes in Eastern and Southern Africa using validated Landsat and MODIS data. Int J Appl Earth Observ Geoinf 62:8–26. https://doi.org/10.1016/j.jag.2017.04.007

Berrisford P et al (2011) Atmospheric conservation properties in ERA-Interim. Q J R Meteorol Soc 137:1381–1399

Bowling LC, Lettenmaier DP (2010) Modeling the effects of lakes and wetlands on the water balance of arctic environments. J Hydrometeorol 11(2):276–295

Bowling LC, Pomeroy JW, Lettenmaier DP (2004) Parameterization of blowing-snow sublimation in a macroscale hydrology model. J Hydrometeorol 5(5):745–762

Brovkin V, Sitch S, von Bloh W, Claussen M, Bauer E, Cramer W (2004) Role of land cover change for atmospheric CO2 increase and climate change during the last 150 years. Glob Chang Biol 10:1253–1266

Burn DH (1997) Catchment similarity for regional flood frequency analysis using seasonality measures. J Hydrol 202:212–230

Clay DE et al (2016) Does the U.S. cropland data layer provide and accurate benchmark for land-use change estimates? Agron J 108:266–272

Cong Thanh N, Singh B (2006) Trend in rice production and export in Vietnam. Omonrice 14:11–123

Costa-Cabral MC et al (2008) Landscape structure and use, climate, and water movement in the Mekong River Basin. Hydrol Process 22:1731–1746

Costenbader J, Broadhead JS, Yasmi Y, Durst PB (2015a) Drivers affecting forest change in the GMS: an overview. FAO/USAID LEAF, Sept 2015

Costenbader J, Varns T, Vidal A, Stanley L, Broadhead JS (2015b) Drivers of forest change in the greater Mekong subregion. Regional Report, FAO/USAID LEAF, Sept 2015

Cuo L et al (2011) Effects of mid-twenty-first century climate and land cover change on the hydrology of the Puget Sound basin, Washington. Hydrol Process 25:1729–1753

Danielson JJ, Gesch DB (2011) Global Multi-resolution Terrain Elevation Data 2010 (GMTED2010). Open File Report, US Geological Survey, Reston

Decker M et al (2012) Evaluation of the reanalysis products from GSFC, NCEP, and ECMWF using flux tower observations. J Clim 25:1916–1943

Dee DP et al (2011) The ERA-Interim reanalysis: configuration and performance of the data assimilation system. Q J R Meteorol Soc 137:553–597

Dobson JE et al (2000) A global population database for estimating populations at risk. Photogramm Eng Remote Sens 66(7):849–857

Dudgeon D (2000) Large-scale hydrological changes in tropical Asia: prospects for riverine biodiversity. Bioscience 50:793–806

Dwarakish GS, Ganasri BP (2015) Impact of land use change on hydrologic systems: a review of current modeling approaches. Cogent Geosci 1:1115691

Eastham J et al (2008) Mekong river basin water resource assessment: impacts of climate change. Technical Report, CSIRO

ECMWF (European Centre for Medium-Range Weather Forecasts) (2009) (updated monthly) ERA-Interim Project. Research Data Archive at the National Center for Atmospheric Research, Computational and Information Systems Laboratory. https://doi.org/10.5065/D6CR5RD9. Accessed 31 Mar 2016

Fernandes R, Leblanc SG (2005) Parametric (modified least squares) and non-parametric (Theil-Sen) linear regressions for predicting biophysical parameters in the presence of measurement errors. Remote Sens Environ 95:303–316

Foody GM (2002) Status of land cover classification accuracy assessment. Remote Sens Environ 80:185–201

Francisco HA (2008) Adaptation to climate change—needs and opportunities in Southeast Asia. ASEAN Econ Bull 25(1):7–19

Friedl MA et al (2010) MODIS Collection 5 global land cover: algorithm refinements and characterization of new datasets. Remote Sens Environ 114:168–182

Funk C et al (2015) The climate hazards infrared precipitation with stations—a new environmental record for monitoring extremes. Sci Data 2:150066

Godin R (2014) Joint Polar Satellite System (JPSS) VIIRS Surface Type Algorithm Theoretical Basis Document (ATBD). Algorithm Theoretical Basis Document (last access: 3 January 2017). https://www.star.nesdis.noaa.gov/jpss/documents/ATBD/D0001-M01-S01-024_JPSS_ATBD_VIIRSSurface-Type_A.pdf

Haddeland I, Lettenmaier DP, Skaugen T (2006a) Effects of irrigation on the water and energy balances of the Colorado and Mekong river basin. J Hydrol 324:210–223

Haddeland I, Skaugen T, Lettenmaier DP (2006b) Anthropogenic impacts on continental surface water fluxes. Geophys Res Lett 33(8):L08406

Hijmans RJ et al (2005) Very high resolution interpolated climate surfaces for global land areas. Int J Climatol 25:1965–1978

Ito A (2007) Simulated impacts of climate and land-cover change on soil erosion and implications for the carbon cycle, 1901 to 2100. Geophys Res Lett 34:L09403

Justice CO et al (2013) Land and cryosphere products from Suomi NPP VIIRS: overview and status. Geophys Res Lett 118:9753–9765

Keskinen M et al (2010) Climate change and water resources in the Lower Mekong River Basin: putting adaptation into the context. J Water Clim Chang 1:103–117

Kibria KN, Ahiablame L, Hay C, Djira G (2016) Streamflow trends and responses to climate variability and land cover change in South Dakota. Hydrology 3

Kingston DG, Thompson JR, Kite G (2011) Uncertainty in climate change projections of discharge for the Mekong River Basin. Hydrol Earth Syst Sci 15:1459–1471

Kite G (2001) Modelling the Mekong: hydrological simulation for environmental impact studies. J Hydrol 253:1–13

Kityuttachai K, Heng S, Sou V (2016) Land cover map of the Lower Mekong Basin, MRC Technical Paper No. 59, Information and Knowledge Management Programme. Mekong River Commission, Phnom Penh, Cambodia

Kummu M, Sarkkula J (2008) Impact of the Mekong river flow alteration on the Tonle Sap flood pulse. Ambio 37(3):185–192

Kummu M, Sarkkula J, Koponen J, Nikula J (2006) Ecosystem management of Tonle Sap Lake: integrated modelling approach. Int J Water Resour Dev 22(3):497–519

Lamberts D (2008) Little impact, much damage: the consequences of Mekong River flow alterations for the Tonle Sap ecosystem. In: Kummu M, Keskinen M, Varis O (eds) Modern myths of the Mekong—a critical review of water and development concepts, principles and policies. Water & Development Publications—Helsinki University of Technology, Espoo, pp 3–18

Lauri H et al (2012) Future changes in Mekong River hydrology: impact of climate change and reservoir operation on discharge. Hydrol Earth Syst Sci 16:4603–4619

Liang X, Lettenmaier DP, Wood EF, Burges SJ (1994) A simple hydrologically based model of land surface water and energy fluxes for general circulation models. J Geophys Res 99:14415–14428

Liu M, Adam JC, Hanlet AF (2013a) Spatial-temporal variations of evapotranspiration and runoff/precipitation ratios responding to the changing climate in the Pacific Northwest during 1921-2006. J Geophys Res Atmos 118:380–394. https://doi.org/10.1029/2012JD018400

Liu X, Liu W, Xia J (2013b) Comparison of the streamflow sensitivity to aridity index between the Danjiangkou Reservoir basin and Miyun Reservoir basin, China. Theor Appl Climatol 111:683–691. https://doi.org/10.1007/s00704-012-0701-3

Liu Y, Li Y, Li S, Motesharrei S (2015) Spatial and temporal patterns of global NDVI trends: correlations with climate and human factors. Remote Sens 7:13233–13250. https://doi.org/10.3390/rs71013233

Lohmann D, Nolte-Holube R, Raschke E (1996) A large-scale horizontal routing model to be coupled to land surface parametrization schemes. Tellus 48:708–721

Lohmann D, Raschke E, Nijssen B, Lettenmaier DP (1998) Regional scale hydrology: I. Formulation of the VIC-2L model coupled to a routing model. Hydrol Sci J 43:131–141

Loveland TR, Belward AS (1997) The IGBP-DIS global 1 km land cover data set, DISCover: first results. Int J Remote Sens 18:3289–3295

LP DAAC (Land Processes Distributed Active Archive Center) (2010) MCD12Q1. V051, NASA EOSDIS Land Processes DAAC, USGS Earth Resources Observation and Science (EROS) Center, Sioux Falls. https://lpdaac.usgs.gov. Accessed 14 Feb 2016

Matheussen B et al (2000) Effects of land cover change on streamflow in the interior Columbia basin. Hydrol Process 14:867–885

Milne R, Jallow BP (2003) Basis for consistent representation of land areas. In: Apps M, Miguez JD (eds) IPCC good practice guidance for LULUCF. pp 2.1–2.29

Moriasi DN et al (2007) Model evaluation guidelines for systematic quantification of accuracy in watershed simulations. Trans ASABE 50:885–900

MRC (Mekong River Commission) (2010) State of the Basin Report: 2010. Mekong River Commission, Vientiane Lao PDR

MRC (Mekong River Commission) (2011) Hydrological database. Mekong River Commission, Vientiane Lao PDR

Nachergaele F, van Vilthuizen H, Verelst L, Wiberg D (2012) Harmonized World Soil Database. Technical Document, United Nations FAO

Nagaraj MK, Yaragal SC (2008) Sensitivity of land cover parameter in runoff estimation using GIS. ISH J Hydraul Eng 14:41–51. https://doi.org/10.1080/09715010.2008.10514891

Nash JE, Sutcliffe JV (1970) River flow forecasting through conceptual models part I—discussion of principles. J Hydrol 10:282–290

Nijssen B, O'Donnell GM, Hamlet AF, LettenMaier DP (2001a) Hydrologic sensitivity of global rivers to climate change. Clim Chang 50:143–175

Nijssen B, Schnur R, Lettenmaier DP (2001b) Global retrospective estimation of soil moisture using the variable infiltration capacity land surface model, 1980–93. J Clim 14:1790–1808

Nijssen B et al (2001c) Predicting the discharge of global rivers. J Clim 14:3307–3323

NOAA CLASS (National Oceanic and Atmospheric Administration Comprehensive Large Array-Data Stewardship System) (2013) VIIRS Surface Type EDR (VSTYO), NOAA CLASS, NOAA Center for Satellite Applications and Research, College Park, Maryland, https://www.class.ncdc.noaa.gov. Accessed 18 July 2016

Olofsson P et al (2014) Good practices for estimating area and assessing accuracy of land change. Remote Sens Environ 148:42–57. https://doi.org/10.1016/j.rse.2014.02.015

Parajka J et al (2009) Comparative analysis of the seasonality of hydrological characteristics in Slovakia and Austria. Hydrol Sci J 54:456–473

Pech S, Sunada K (2008) Population growth and natural-resources pressure in the Mekong River Basin. Ambio 37:219–224

Peel MC, Finlayson BL, McMahon TA (2007) Updated world map of the Koppen-Geiger climate classification. Hydrol Earth Syst Sci 11:1633–1644. https://doi.org/10.5194/hess-11-1633-2007

Pontius RG Jr, Schneider LC (2001) Land-cover change model validation by an ROC method for the Ipswich watershed, Massachusetts, USA. Agric Ecosyst Environ 85:239–248

Prathumratana L, Sthiannopkao S, Kim KW (2008) The relationship of climate and hydrologic parameters to surface water quality in the lower Mekong River. Environ Int 34:860–866. https://doi.org/10.1016/j.envint.2007.10.011

Ratnam J et al (2011) When is a 'forest' a savanna, and why does it matter? Glob Ecol Biogeogr 20:1–8. https://doi.org/10.1111/j.1466-8238.2010.00634.x

Romanic D, Curic M, Jovicic I, Lompar M (2015) Long-term trends of the 'Koshava' wind during the period 1949-2010. Int J Climatol 35:288–302. https://doi.org/10.1002/joc.3981

Sakamoto T et al (2006) Spatio-temporal distribution of rice phenology and cropping systems in the Mekong Delta with special reference to the seasonal water flow of the Mekong and Bassac rivers. Remote Sens Environ 100:1–16

Schaake JC (1990) From climate to flow. In: Waggoner PE (ed) Climate change and U.S. water resources. Wiley, New York, pp 177–206

Sen PK (1968) Estimates of the regression coefficient based on Kendall's tau. J Am Stat Assoc 63:1379–1389

Stehman SV (1996) Estimating the Kappa coefficient and its variance under stratified random sampling. Photogramm Eng Remote Sens 62:401–407

Strahler A et al (1999) MODIS land cover product algorithm theoretical basis document (ATBD) Version 5.0. Technical Document, NASA. https://modis.gsfc.nasa.gov/data/atbd/atbd_mod12.pdf

Tatsumi K, Yamashiki Y (2015) Effect of irrigation water withdrawals on water and energy balance in the Mekong River Basin using an improved VIC land surface model with fewer calibration parameters. Agric Water Manag 159:92–106. https://doi.org/10.1016/j.agwat.2015.05.011

Thompson JR, Green AJ, Kingston DG, Gosling SN (2013) Assessment of uncertainty in river flow projections for the Mekong River using multiple GCMs and hydrological models. J Hydrol 486:1–30. https://doi.org/10.1016/j.jhydrol.2013.01.029

Tote C et al (2015) Evaluation of satellite rainfall estimates for drought and flood monitoring in Mozambique. Remote Sens 7:1758–1776. https://doi.org/10.3390/rs70201758

Trenberth KE, Fasullo JT, Mackaro J (2011) Atmospheric moisture transports from Ocean to land and global energy flows in reanalyses. J Clim 24:4907–4924. https://doi.org/10.1175/2011JCLI1471.1

Verburg PH et al (2002) Modeling the spatial dynamics of regional land use: the CLUE-S model. Environ Manag 30:391–405. https://doi.org/10.1007/s00267-002-2630-x

Wijesekara GN et al (2012) Assessing the impact of future land-use changes on hydrological processes in the Elbow River watershed in southern Alberta, Canada. J Hydrol 412:220–232

Zheng J, Yu X, Deng W, Wang H, Wang Y (2013) Sensitivity of land-use change to stream-flow in Chaobai river basin. J Hydrol Eng 18:457–464. https://doi.org/10.1061/(ASCE)HE.1943-5584.0000669